BASS CONSTRUCTION WITH MULTI-MARGINALS: LIGHTSPEED COMPUTATION IN A NEW LOCAL VOLATILITY MODEL

ANTOINE CONZE AND PIERRE HENRY-LABORDÈRE

May 25, 2021

Abstract. The local volatility model [5] is widely used as this is the unique one-factor Markov model perfectly calibrated to a continuum of vanilla options in strike and expiry. It requires unfortunately an arbitrage-free interpolation of implied volatility in expiry and a time-consuming Euler discretization scheme for its simulation. In this paper, we construct a new local volatility model, based on the extension of the Bass construction [1], which is (1) perfectly calibrated to vanilla options on market expiries and (2) is also a one-factor diffusion which can be discretized exactly as it requires only the simulation of a standard Brownian motion, providing very fast calculations.

Introduction

Let us consider an horizon T, the non-negative spot price process $(S_t)_{0\leq t\leq T}$, and the convex set of martingale measures[1]

$$\mathcal{M}_n := \{\mathbb{P} \ / \ (S_t)_{0\leq t\leq T} \text{ martingale under } \mathbb{P}, \quad S_{T_i} \overset{\mathbb{P}}{\sim} \mu_i, \quad i = 1, \cdots, n\}$$

fitting discrete marginals $(\mu_i)_{1\leq i\leq n}$ supported in $\mathbb{R}_+$. These marginals $(\mu_i)_{1\leq i\leq n}$ are implied in practice from market prices of vanilla options with expiries $0 := T_0 < T_1 < \cdots < T_n := T$. In order to get an non-empty set, we assume that $\mu_1 < \cdots < \mu_n$ are ordered in the convex sense[2] from Kellerer's theorem [11].

Various arbitrage-free models belonging to $\mathcal{M}_n$ have been built in the past (see [9], Chapter 4 for an overview). Unfortunately, most of these models require a time-interpolation of the implied volatility, which can lead to some difficulties, and the numerical calibration to vanilla options can be tricky. One can cite the Dupire local volatility model [5], local stochastic volatility models and local Lévy's models [3] having a local compensator depending on the time and S_t.

For examples of models fitting directly discrete marginals, one can cite the local variance Gamma model [4] and the martingale Schrödinger bridges [10]. In this paper, we introduce a new local volatility model based on an extension of the Bass construction [1], that we denote Bass-LV. This model is calibrated exactly to discrete marginals. In short, the underlying process $(S_t)_{0\leq t\leq T}$ is obtained as an explicit function $S_t = f(t, W_t)$ of the time t and a predictable RCLL process $(W_t)_{0\leq t\leq T}$ such that $W_t = W_{T_i} + B_t - B_{T_i} \ \ \forall t \in [T_i, T_{i+1}), \forall i = 0, \cdots, n-1$, with $(B_t)_{0\leq t\leq T}$ a

[1] For the sake of simplicity, we will assume no dividends, zero repo and interest rate so that the spot price is a martingale. As is well known (see for instance [8]), cash/yield dividends and non-zero repo and interest rate can be included by introducing a continuous positive local martingale X_t defined by $S_t = A(t)X_t + B(t)$ where the two functions $A > 0$ and B depend on the cash/yield discrete dividends, repo and interest rate. Market vanilla options on S_t with strike K map into $A(t)$ vanilla options on X_t with strike $(K - B(t))/A(t)$, and the model is then built for the process $(X_t)_{0\leq t\leq T}$.

[2] $\mu_i \overset{\text{convex}}{<} \mu_{i+1}$ means that $\mathbb{E}[(S_{T_i} - K)^+] < \mathbb{E}[(S_{T_{i+1}} - K)^+]$ for all K.

standard Brownian motion and $W_{T_i} = f^{-1}(T_i, f(T_i^-, W_{T_i^-}))$. [3] It can therefore (1) be simulated exactly and (2) its overall complexity is that of a standard Brownian motion. In the limit of continuous-time marginals when the number of expiries n increases and $\max_{0\leq i\leq n-1}(T_{i+1} - T_i)$ goes to zero, our model converges to the Dupire local volatility model [5].

The contents of our paper is as follows. We recall in the first section the Bass construction (with one marginal), which is close in spirit to the Markov functional model used in fixed-income. Then, we present our multi-marginal extension. The numerical procedure for computing the mapping f is done using a fixed-point method which converges quickly. We also present an AD inspired algorithm for computing volatility greeks. In the final section, we extend our construction by fitting a future skew or including a stochastic volatility.

This work was originated when the second author was visiting the Oxford mathematical institute in July 2019. He would like to thank Prof. Rama Cont and Prof. Jan Obłój for their kind hospitality.

1. Bass Construction With One Marginal [1]: A Reminder

We assume that the non-negative martingale $(S_t)_{0\leq t\leq T_1}$ can be written as $S_t = f(t, W_t)$ where $(W_t)_{0\leq t\leq T_1}$ is a standard Brownian motion (with $W_0 := 0$) and the mapping f is such that $S_{T_1} \sim \mu_1$. The conditions are:

(a) The martingale property imposes that f is a solution of the heat kernel equation:

$$\partial_t f + \frac{1}{2}\partial_w^2 f = 0$$

(b) The marginal constraint $S_{T_1} \sim \mu_1$ fixes the terminal condition $f(T_1, \cdot)$:

$$f(T_1, w) = F_{\mu_1}^{-1} \circ \mathcal{N}\left(\frac{w}{\sqrt{T_1}}\right)$$

where $\mathcal{N}$ is the Gaussian cumulative distribution. Consequently, for all $t \in [0, T_1]$, the function $f(t, \cdot)$ can be written as the convolution of $f(T_1, \cdot)$ with the heat kernel $K_t(x) := e^{-\frac{x^2}{2t}}/\sqrt{2\pi t}$:

$$f(t, \cdot) = K_{T_1-t} \star f(T_1, \cdot) = K_{T_1-t} \star \left(F_{\mu_1}^{-1} \circ \mathcal{N}\left(\frac{\cdot}{\sqrt{T_1}}\right)\right)$$

Here $\circ$ denotes the composition operator and $\star$ the convolution.

2. Bass Construction With 2 Marginals: Fitting Vanilla Options At T_1 And T_2

As above, we set $S_t = f(t, W_t)$ for all $t \in [T_1, T_2]$, where $(W_t)_{T_1\leq t\leq T_2}$ is now defined as $W_t = W_{T_1} + B_t - B_{T_1}$ with W_{T_1} a random variable and $(B_t)_{T_1\leq t\leq T_2}$ a Brownian motion independent of W_{T_1}.

We construct the mapping f and the law of W_{T_1} such that **(a)** $(S_t)_{T_1\leq t\leq T_2}$ is a non-negative martingale, **(b)** $S_{T_2} \sim \mu_2$ and **(c)** $S_{T_1} \sim \mu_1$. These conditions will fix uniquely f and the law of W_{T_1}. Let us emphasize that in general W_{T_1} is not distributed as a Brownian motion evaluated at T_1.

In mathematical finance terminology, the resulting process $(S_t)_{T_1\leq t\leq T_2}$ corresponds to an arbitrage-free model calibrated to T_1 and T_2-vanilla options. This construction can be trivially extended to the case where we fit n discrete-time marginals ordered in the convex order as will be seen in the next section 3.1. This model defines a nice alternative to the Dupire local volatility model

[3] For clarity, throughout the paper we use the notation $f^{-1}(t, x) := (f(t, .))^{-1}(x)$

[5] as (1) it does not require to construct a continuous-time implied volatility surface and (2) its numerical implementation requires only the (exact and fast) simulation of a standard Brownian motion. This construction is different from [2], although close.

We denote $(F_{\mu_i})_{i=1,2}$ the cumulative distributions of $(\mu_i)_{i=1,2}$ and $F_{W_{T_1}}$ the cumulative distribution of the law of W_{T_1}. We assume that $\mu_1 \overset{\text{convex}}{<} \mu_2$ and for the sake of simplicity that $(\mu_i)_{i=1,2}$ are smooth, compactly supported and strictly positive. This technical condition is needed in our proofs. In practice, marginals are implied from a finite number of strikes and could be interpolated/extrapolated in order to satisfy this condition.

Our main result is

Theorem 2.1. **(a)** *$(S_t)_{T_1 \le t \le T_2}$ is a martingale,* **(b)** *$S_{T_2} \sim \mu_2$ and* **(c)** *$S_{T_1} \sim \mu_1$ if and only if $F_{W_{T_1}}$ satisfies the fixed-point equation*

$$F_{W_{T_1}} = \mathcal{A}\, F_{W_{T_1}} \tag{1}$$

where the non-linear integral operator $\mathcal{A}$ is defined by:

$$\mathcal{A}F := F_{\mu_1} \circ \left(K_{T_2-T_1} \star \left(F_{\mu_2}^{-1} \circ (K_{T_2-T_1} \star F)\right)\right) \tag{2}$$

The function $f(t,\cdot)$ for $t \in [T_1, T_2]$ is then

$$f(t,\cdot) = K_{T_2-t} \star \left(F_{\mu_2}^{-1} \circ \left(K_{T_2-T_1} \star F_{W_{T_1}}\right)\right) \tag{3}$$

where $F_{\mu_i}^{-1}(u) := \inf\{x \;:\; F_{\mu_i}(x) \ge u\}, \quad u \in [0,1]$.

All the proofs are reported in the appendix. At this point, we need to show that there exists a solution to (1). First, we have the result:

Lemma 2.2. *$\mathcal{A}(\mathcal{E}) \subset \mathcal{E}$ where $\mathcal{E}$ is the space of cumulative distributions (i.e., non-decreasing right-continuous functions $F : \mathbb{R} \to [0,1]$ with $\lim_{x\to-\infty} F(x) = 0$ and $\lim_{x\to\infty} F(x) = 1$).*

Remark 2.3. **(1)** *Let us remark that $\mathcal{A}$ is a monotone operator, resulting from the monotonicity of $K_\cdot$ and the two functions F_{μ_1}, F_{μ_2}: if $F_1 < F_2$ then $\mathcal{A}F_1 < \mathcal{A}F_2$.*

(2) *If F is a solution of the fixed-point equation (2), then also $F(\cdot + c)$ with c an arbitrary constant. This shift by an constant is irrelevant in our construction as it corresponds to replacing the random variable W_{T_1} by $W_{T_1} + c$. By construction we will set $F_{W_{T_1}}(0) := \frac{1}{2}$.*

Theorem 2.4 (Existence)**.** *There exists a fixed-point to $\mathcal{A}F_{W_{T_1}} = F_{W_{T_1}}$ in $\mathcal{E}$.*

By expanding equation (1) at the first-order in $\Delta := T_2 - T_1$ using $K_\Delta \star F \approx F + \frac{1}{2}\Delta F''$, we get a second-order ODE satisfied by $F_{W_{T_1}}$:

$$G_2(F(w)) + \Delta G_2'(F(w))F''(w) + \frac{1}{2}\Delta F'(w)^2 G_2''(F(w)) = G_1(F(w)) \tag{4}$$

where $G_i(y) := F_{\mu_i}^{-1}(y)$, $i = 1,2$. We state an uniqueness result for this linearized equation which uses naturally the convex-order condition. This indicates that a new clever proof should establish the uniqueness for the non-linearized fixed point equation (1).

Proposition 2.5 (Uniqueness for the linearized fixed-point equation)**.** *There exists a unique solution in $\mathcal{E}$ (up to the transformation Remark 2.3 -* **(2)***) to the ODE (4).*

Remark 2.6 (Link with the Black-Scholes model). *As mentioned above, W_{T_1} is not distributed as a Brownian motion evaluated at T_1, except in the case where μ_1 and μ_2 are log-normal distributions with standard deviations of log respectively $\sigma\sqrt{T_1}$ and $\sigma\sqrt{T_2}$. In this case, the solution to the fixed point (1) is $F_{W_{T_1}} = \mathcal{N}\left(\frac{\cdot}{\sqrt{T_1}}\right)$ and $f(t,w) = S_0 \exp(-\frac{1}{2}\sigma^2 t + \sigma w)$. In this short, when applied to log-normal distributions, our construction yields the Black-Scholes model.*

3. A New local volatility model: Bass-LV model

3.1. **Fitting Vanillas at all market expiries.** Let us assume that we have n marginals implied from market prices of call options of maturities $0 := T_0 < T_1 < \cdots < T_n := T$. We denote $f_{[T_i,T_{i+1}]}$ the mapping built from the previous section 2 using the marginals μ_i and μ_{i+1} for all $i = 1, \cdots, n-1$, and $f_{[0,T_1]}$ the mapping built from the classical Bass construction outlined in Section 1. Let $i(t) := \sup\{i < n / T_i \leq t\}$ and $(B_t)_{0\leq t\leq T}$ be a standard Brownian motion. We set $S_t = f(t, W_t)$ where the mapping f is defined as

$$f(t,\cdot) := f_{[T_{i(t)},T_{i(t)+1}]}(t,\cdot) \tag{5}$$

and the predictable RCLL process $(W_t)_{0\leq t\leq T}$ is

$$W_t = W_{T_{i(t)}} + B_t - B_{T_{i(t)}} \tag{6}$$

with $W_{T_0} := 0$ and the $(W_{T_i})_{1\leq i\leq n-1}$ obtained from the continuity condition for the spot price at each T_i

$$S_{T_i^-} := f(T_i^-, W_{T_i^-}) = f(T_i, W_{T_i}) := S_{T_i} \tag{7}$$

which we can rewrite as (see footnote 3)

$$W_{T_i} = f^{-1}(T_i, f(T_i^-, W_{T_i^-})) \tag{8}$$

It is straightforward to check that **(a)** $(S_t)_{0\leq t\leq T}$ is a martingale and **(b)** $S_{T_i} \sim \mu_i$ for all $i = 1, \cdots, n$.

3.2. **A new local volatility.** The dynamics for all $t \in [T_i, T_{i+1})$ is then:

$$\begin{aligned}\frac{dS_t}{S_t} &= \partial_w \ln f_{[T_i,T_{i+1}]}(t, W_{T_i} + B_t - B_{T_i}) dB_t \\ &= \partial_w \ln f_{[T_i,T_{i+1}]}(t, f^{-1}_{[T_i,T_{i+1}]}(t,S_t)) dB_t := \sigma_i(t,S_t) dB_t\end{aligned}$$

This corresponds to a local volatility $\sigma(t,S) = \sigma_{i(t)}(t,S)$, so the Bass-LV model is indeed a local volatility model calibrated to the market expiries $(T_i)_{1\leq i\leq n}$. Unlike the Dupire local volatility model, it does not require an arbitrage-free interpolation of the implied volatility in expiry, and in fact leads to a simple arbitrage-free interpolation in time of the marginals $(\mu_i)_{1\leq i\leq n}$.

3.3. **Multi-asset case.** Consider two underlyings $(S_t^1)_{0\leq t\leq T}$ and $(S_t^2)_{0\leq t\leq T}$, each with its own Bass-LV model $S_t^1 = f^1(t, W_t^1)$ and $S_t^2 = f^2(t, W_t^2)$. Then

$$\langle dS_t^1, dS_t^2 \rangle = \partial_{w^1} f^1(t, W_t^1) \partial_{w^2} f^2(t, W_t^2) \langle dB_t^1, dB_t^2 \rangle$$

and the instantaneous correlation between dS_t^1 and dS_t^2 is the same as the correlation between dB_t^1 and dB_t^2. Therefore, the break-even correlation for the Bass-LV and Dupire-LV models coincide.

3.4. **Numerics.**

3.4.1. *Numerical calibration: algorithm.* Let $\mathcal{A}_i$ denote the non-linear integral operator in Theorem 2.1 when applied to the marginals μ_i and μ_{i+1}. The numerical algorithm for building the mapping $f_{[T_i,T_{i+1}]}$ can be described by the following steps:

(1) Set $F^{(0)}_{W_{T_i}}$ as given by the solution of the linearized fixed-point (4) (see equation 26).

(2) Iterate until convergence the equation:

$$F^{(p+1)}_{W_{T_i}} = \mathcal{A}_i F^{(p)}_{W_{T_i}}$$

Although we have not shown that $\mathcal{A}$ is a contraction, we will illustrate in our numerical examples that the above iteration converges quickly in the $\mathrm{Ł}^\infty$-norm.

(3) The mapping $f_{[T_i,T_{i+1}]}$ at any time $t \in [T_i, T_{i+1}]$ is then

$$f_{[T_i,T_{i+1}]}(t,\cdot) = K_{T_{i+1}-t} \star \left(F^{-1}_{\mu_{i+1}} \circ \left(K_{T_{i+1}-T_i} \star F^{(\infty)}_{W_{T_i}}\right)\right)$$

For practical purposes, all one-dimensional functions are stored and evaluated as linear or spline interpolations, and convolution with the heat kernel is done using a Gauss–Hermite quadrature. The construction of each $f_{[T_i,T_{i+1}]}$ is independent of the others, so that the algorithm could be parallelized.

3.4.2. *Monte-Carlo simulation: algorithm.* Consider a set of ordered simulation dates $0 := t_0 < t_1 < \cdots < t_m$ that contains the calibration dates $(T_i)_{0\le i\le n}$. The MC simulation algorithm of a sample path along the simulation dates is a large step scheme that works as follows (we recall that $i(t) := \sup\{i < n / T_i \le t\}$):

- start from S_0 and $W_0 := 0$
- large step to t_1:
  - draw a Gaussian G_1 and set $W_{t_1^-} := \sqrt{t_1} G_1$
  - if t_1 is not a market date, set $W_{t_1} := W_{t_1^-}$ and $S_{t_1} := f(t_1, W_{t_1})$
  - if t_1 is a market date $T_{i(t_1)}$, set $S_{t_1} = S_{t_1^-} := f(T^-_{i(t_1)}, W_{t_1^-})$ and $W_{t_1} := f^{-1}(T_{i(t_1)}, S_{t_1})$
- large step to t_2:
  - draw a Gaussian G_2 and set $W_{t_2^-} := W_{t_1} + \sqrt{t_2 - t_1} G_2$
  - if t_2 is not a market date, set $W_{t_2} := W_{t_2^-}$ and $S_{t_2} := f(t_2, W_{t_2})$
  - if t_2 is a market date $T_{i(t_2)}$, set $S_{t_2} = S_{t_2^-} := f(T^-_{i(t_2)}, W_{t_2^-})$ and $W_{t_2} := f^{-1}(T_{i(t_2)}, S_{t_2})$
- ...

Example 3.1. *To illustrate the simulation algorithm, consider an exotic with three fixings in $t_1^f = 0.5$ months, $t_2^f = 1.5$ months and $t_3^f = 3.5$ months, with hypothetical market dates $T_1 = 1$ week, $T_2 = 1$ month, $T_3 = 3$ months. The set of simulation dates is $(t_k)_{0\le k\le 6} := \{0, T_1, t_1^f, T_2, t_2^f, t_3^f, T_3\}$.*

- *large step to T_1 (market date): draw a Gaussian G_1 and set $W_{T_1^-} := \sqrt{t_1} G_1$, then $S_{T_1} = S_{T_1^-} := f_{[T_0,T_1]}(T_1, W^-_{T_1})$ and $W_{T_1} := f^{-1}_{[T_1,T_2]}(T_1, S_{T_1})$.*
- *large step to t_1^f (not a market date): draw a Gaussian G_2 and set $W_{t_1^f} := W_{T_1} + \sqrt{t_1^f - T_1} G_2$ and $S_{t_1^f} := f_{[T_1,T_2]}(t_1^f, W_{t_1^f})$.*

- *large step to T_2 (market date): draw a Gaussian G_3 and set $W_{T_2^-} := W_{t_1^f} + \sqrt{T_2 - t_1^f}G_3$, then $S_{T_2} = S_{T_2^-} := f_{[T_1,T_2]}(T_2, W_{T_2}^-)$ and $W_{T_2} := f^{-1}_{[T_2,T_3]}(T_2, S_{T_2})$.*
- *large step to t_2^f (not a market date): draw a Gaussian G_4 and set $W_{t_2^f} := W_{T_2} + \sqrt{t_2^f - T_2}G_4$ and $S_{t_2^f} := f_{[T_2,T_3]}(t_2^f, W_{t_2^f})$.*
- *large step to t_3^f (not a market date): draw a Gaussian G_5 and set $W_{t_3^f} := W_{t_2^f} + \sqrt{t_3^f - t_2^f}G_5$ and $S_{t_3^f} := f_{[T_2,T_3]}(t_3^f, W_{t_3^f})$.*

For a pricing of a 10Y exotic derivative with annual fixing dates, with the calibration algorithm on a dozen market expiries, we have found that our model is up to *80* times faster than pricing with the Dupire local volatility model and a daily Euler discretization (see Tables 1 and 2).

4. Numerical examples

4.1. **Fitting Vanilla Options.** We consider the SX5E market smile (April 29, 2021). Once the mapping functions are obtained, we recompute Vanilla options by Monte-Carlo simulation – see Section 3.4.2. We observe a perfect match (See Figure 1, left), with an error less than a few bps, the largest for deep OTM options. The fixed-point algorithm converges quickly, even when starting from a naive Brownian distribution for $F^{(0)}_{W_{T_i}} := \mathcal{N}\left(\frac{\cdot}{\sqrt{T_i}}\right)$ (See Figure 1, right).

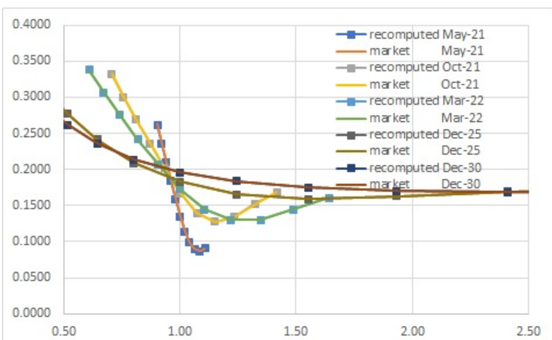

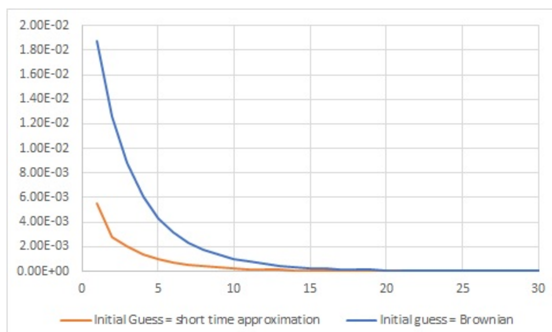

Figure 1. Left: Calibration to market smile for various expiries, as a function of moneyness. Right: Convergence of the $\|F^{(p)}_{W_{T_i}} - F^{(p-1)}_{W_{T_i}}\|_\infty$ for the Dec 25 expiry as a function of the iteration (p).

4.2. **Dupire-LV versus Bass-LV construction: The Case of Exotic Options.** Our model, characterized by the martingale measure $\mathbb{P}^\Delta$, where $\Delta := \max_{1\le i\le n}(T_i - T_{i-1})$, is one-factor, continuous and belongs to $\mathcal{M}_n$. As the Dupire local volatility model, denoted by the martingale measure $\mathbb{P}^{\mathrm{LV}}$, is the unique Markov one-dimensional model calibrated to continuous-time marginals $(\mu_t)_{t\in[0,T]}$, this implies by uniqueness that if we increase the number n of calibrated expiries such that $\Delta \to 0$, we get

$$\lim_{\Delta\to 0} \mathbb{P}^\Delta = \mathbb{P}^{\mathrm{LV}}$$

where the limit is understood in the weak sense. In practice, Δ is around one year and therefore we suspect that our discrete local volatility model should be close to the local volatility model.

4.2.1. *Forward-start options.* We have numerically illustrated this statement by computing prices for forward-start options $\mathbb{E}[(\frac{S_{T_{i+1}}}{S_{T_i}} - K)^+]$ for various pair of consecutive expiries, again for the SX5E as of April 29, 2021. The prices are quoted in terms of an (forward) implied volatility as a function of the strike K. We can see a perfect match (See Figure 2). An interesting question could be to quantify the Wasserstein distance between $\mathbb{P}^{\mathrm{LV}}$ and $\mathbb{P}^{\Delta}$.

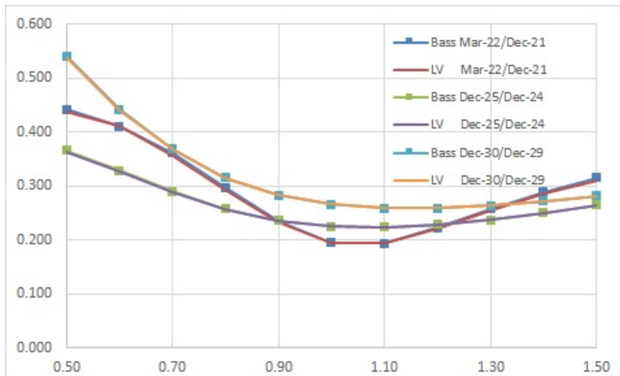

FIGURE 2. $\mathbb{E}[(\frac{S_{T_{i+1}}}{S_{T_i}} - K)^+]$ for various pair of consecutive expiries as a function of strike K: Multi-marginal Bass versus LV model (SX5E, April 29, 2021).

We have also experimented with various exotic structures such as Autocalls, Lookback options, Asian options, etc. and have found that prices with our Bass-LV model and with the Dupire-LV model agree to a difference of no more than a few bps.

4.2.2. *Autocalls.* Below we show results for a 10Y Autocall with yearly call dates, recall barrier 100 and Put-Down-In barrier 70, incremental coupon 5, and for a 10Y Asian option with yearly fixings and strike 100, using the SX5E market smile on April 29, 2021.

	Price	Pricing Time
Bass-LV	-4.56	**3** secs (1 sec calib. + 2 secs pricing)
Dupire-LV Euler (daily time steps)	-4.54	240 secs

TABLE 1. 10Y Autocall with yearly call dates, recall barrier 100 and PDI Barrier 70, incremental coupon 5. Pricing uses 2^{19} paths, mono-threaded on a single i7 2 Ghz CPU.

4.2.3. *Asian.* See similar results for Asian options.

	Price	Pricing Time
Bass-LV	-7.83	**3** secs (1 sec calib. + 2 secs pricing)
Dupire-LV Euler (daily time steps)	-7.83	240 secs

TABLE 2. 10Y Asian option with yearly fixings and strike 100.

5. Volatility Greeks: Automatic Differentiation

Let $f_{i+1} = f(T_{i+1}^-, .)$ be the mapping at the end of each interval $[T_i, T_{i+1})$. Recall that the mapping on any $t \in [0, T]$ is given by

$$f(t, .) = K_{T_{i+1}-t} \star f_{i+1}, \;\; T_i \le t < T_{i+1}$$

Given the $(f_i)_{i=1,\cdots,n}$, the model is then entirely defined through equations (5) to (8) in Section 3.1.

Suppose we bump the $(f_i)_{i=1,\cdots,n}$, making sure each remains a non-decreasing function, and that we recompute $f(t, .)$ as above. In order to keep the initial spot price S_0 unchanged we start from $W_0 = f^{-1}(0, S_0)$ instead of $W_0 = 0$. Equations (5) to (8) now define a new arbitrage free model where the spot process is still a martingale with initial value S_0 but with new marginals on the market dates $(T_i)_{i=1,\cdots,n}$. This remark yields the following algorithm for computing the volatility greeks of an (exotic) option :

5.1. **Algorithm in a nutshell.**

(1) compute the (exotic) option price sensitivities to bumps of the $(f_i)_{i=1,\cdots,n}$ when pricing using Monte-Carlo simulation – see Section 5.3. Note that because the spot process is a martingale with fixed mean S_0, the price sensitivities of a linear payoff are zero;

(2) Compute the marginal sensitivities to these bumps, using a semi-analytical approach – see Section 5.4. This will yield the vanilla options sensitivities;

(3) Setup a discrete portfolio of vanilla options that neutralizes the (exotic) option price sensitivities, this will provide the vanilla options hedge of the (exotic) option.

5.2. **Choice of the bumped mappings.** We consider bumped mappings

$$\hat{f}_i(w, b) = f_i(w) + \sum_{l=1}^{L} b_i^l h_i^l(w)$$

with $b = (b_i^l)_{1 \le l \le L}$ the bump sizes and $h_i^l(\cdot)$ the bump functions. For instance we can use simple hat functions

$$h_i^l(w) = \frac{w - w_i^{l-1}}{w_i^l - w_i^{l-1}} \mathbf{1}_{w_i^{l-1} \le w < w_i^l} + \frac{w_i^{l+1} - w}{w_i^{l+1} - w_i^l} \mathbf{1}_{w_i^l \le w < w_i^{l+1}} \tag{9}$$

where the $(w_i^l)_{0 \le l \le L+1}$ are chosen so as to span an area where most of the distribution of W_{T_i} is supported. We will denote $\frac{\partial}{\partial b_i^l}$ the sensitivity to each bump size, computed at $b = 0$. We have $\frac{\partial \hat{f}_i}{\partial b_i^l}(w) = h_i^l(w)$. Since $\hat{f}_i(w)|_{b=0} = f_i(w)$, we will drop the hat notation, and simply write $\frac{\partial f_i}{\partial b_i^l}(w) = h_i^l(w)$. Also for clarity we denote $\tilde{f}_i = f(T_i, .)$ the mapping at the beginning of the interval $[T_i, T_{i+1})$.

Below we explain how to compute the sensitivities in a Monte-Carlo simulation pricing, and how to compute the sensitivities for vanilla options using a semi-analytical approach.

5.3. **MC price sensitivity to bumped mappings.** This is done using AD through a forward sweep then a backward sweep:

Forward sweep. Let $f_w(t,w) := \frac{\partial f}{\partial w}(t,w)$. We compute and store

$$\frac{\partial S_{t_{k+1}}}{\partial S_{t_k}} = \frac{f_w(t_{k+1}^-, W_{t_{k+1}^-})}{f_w(t_k, W_{t_k})}$$

Backward sweep. Let $\Phi := \Phi(S_{t_1}, \cdots, S_{t_n})$ be the (exotic) option payoff and $\overline{S_{t_k}}$ the sensitivity of the path price to S_{t_k}. Then

$$\overline{S_{t_k}} = \frac{\partial \Phi}{\partial S_{t_k}}, \quad \overline{S_{t_k}} += \overline{S_{t_{k+1}}} \frac{\partial S_{t_{k+1}}}{\partial S_{t_k}} \tag{10}$$

Path price sensitivity to b_i^l.

$$\frac{\partial \text{PathPrice}}{\partial b_i^l} = \sum_k \frac{\partial S_{t_k}}{\partial b_i^l} \frac{\partial \Phi}{\partial S_{t_k}} = \sum_{T_{i-1} < t_k < T_i} \frac{\partial S_{t_k}}{\partial b_i^l} \frac{\partial \Phi}{\partial S_{t_k}} + \frac{\partial S_{T_i}}{\partial b_i^l} \overline{S_{T_i}} \tag{11}$$

The first term $\sum_{T_{i-1} < t_k < T_i} \frac{\partial S_{t_k}}{\partial b_i^l} \frac{\partial \Phi}{\partial S_{t_k}}$ in equation (11) follows from the bump b_i^l affecting each S_{t_k} for $T_{i-1} < t_k < T_i$. The second term $\frac{\partial S_{T_i}}{\partial b_i^l} \overline{S_{T_i}}$ follows from the bump affecting S_{T_i} which in turns affects all the S_{t_k} for $t_k \geq T_i$.

We have

$$\begin{aligned}
\frac{\partial S_{t_k}}{\partial b_i^l} &= \frac{\partial f}{\partial b_i^l}(t_k, W_{t_k}) - \frac{\partial \tilde{f}_{i-1}}{\partial b_i^l}(W_{T_{i-1}}) f_w(t_k, W_{t_k}) / \tilde{f}_{i-1}^{'}(W_{T_{i-1}}), \quad T_{i-1} < t_k < T_i \\
\frac{\partial S_{T_i}}{\partial b_i^l} &= \frac{\partial f_i}{\partial b_i^l}(W_{T_i^-}) - \frac{\partial \tilde{f}_{i-1}}{\partial b_i^l}(W_{T_{i-1}}) f_i^{'}(W_{T_i^-}) / \tilde{f}_{i-1}^{'}(W_{T_{i-1}})
\end{aligned}$$

with

$$\frac{\partial f}{\partial b_i^l}(t_k, .) = K_{T_i - t_k} \star \frac{\partial f_i}{\partial b_i^l}, \quad \frac{\partial \tilde{f}_{i-1}}{\partial b_i^l} = K_{T_i - T_{i-1}} \star \frac{\partial f_i}{\partial b_i^l}$$

Note that with the choice of the hat functions (9) for the mapping sensitivities, the quantities $K_\Delta \star \frac{\partial f_i}{\partial b_i^l}$ are computed explicitly as

$$\begin{aligned}
K_\Delta \star \frac{\partial f_i}{\partial b_i^l} = &\frac{w_i^{l+1} - w}{w_i^{l+1} - w_i^l} \left(\mathcal{N}\left(\frac{w_i^{l+1} - w}{\sqrt{\Delta}} \right) - \mathcal{N}\left(\frac{w_i^l - w}{\sqrt{\Delta}} \right) \right) \\
&- \frac{w_i^{l-1} - w}{w_i^{l-1} - w_i^l} \left(\mathcal{N}\left(\frac{w_i^{l-1} - w}{\sqrt{\Delta}} \right) - \mathcal{N}\left(\frac{w_i^l - w}{\sqrt{\Delta}} \right) \right) \\
&+ \frac{\sqrt{\Delta}}{w_i^{l+1} - w_i^l} \left(\mathfrak{n}\left(\frac{w_i^{l+1} - w}{\sqrt{\Delta}} \right) - \mathfrak{n}\left(\frac{w_i^l - w}{\sqrt{\Delta}} \right) \right) \\
&- \frac{\sqrt{\Delta}}{w_i^{l-1} - w_i^l} \left(\mathfrak{n}\left(\frac{w_i^{l-1} - w}{\sqrt{\Delta}} \right) - \mathfrak{n}\left(\frac{w_i^l - w}{\sqrt{\Delta}} \right) \right)
\end{aligned}$$

with $\mathcal{N}(.)$ and $\mathfrak{n}(.)$ respectively the gaussian cdf and density.

5.4. **Semi-Analytical Vanilla calls sensitivity to bumped mappings.** Here the goal is to compute semi-analytically the T_i-vanilla calls sensitivities to the mapping. Let $\Delta_i = T_{i+1} - T_i$, $F_{\mu_i}(S) = \mathbb{P}(S_{T_i} < S)$, $F_{W_{T_i}}(w) = \mathbb{P}(W_{T_i} < w)$ and $F_{W_{T_i^-}}(w) = \mathbb{P}(W_{T_i^-} < w)$. From the model equations (5) to (8) the cumulative distribution functions satisfy the forward induction

$$\begin{aligned} F_{\mu_i} &= F_{W_{T_i^-}} \circ f_i^{-1} \\ F_{W_{T_i}} &= F_{\mu_i} \circ \tilde{f}_i \\ F_{W_{T_{i+1}^-}} &= K_{\Delta_i} \star F_{W_{T_i}} \end{aligned} \tag{12}$$

Differentiating with respect to b_j^l we obtain the forward induction equations

$$\begin{aligned} \frac{\partial F_{\mu_i}}{\partial b_j^l} &= \frac{\partial F_{W_{T_i^-}}}{\partial b_j^l} \circ f_i^{-1} + \left(F'_{W_{T_i^-}} \circ f_i^{-1}\right) \times \frac{\partial f_i^{-1}}{\partial b_j^l} \\ \frac{\partial F_{W_{T_i}}}{\partial b_j^l} &= \frac{\partial F_{\mu_i}}{\partial b_j^l} \circ \tilde{f}_i + \left(F'_{\mu_i} \circ \tilde{f}_i\right) \times \frac{\partial \tilde{f}_i}{\partial b_j^l} \\ \frac{\partial F_{W_{T_{i+1}^-}}}{\partial b_j^l} &= K_{\Delta_i} \star \frac{\partial F_{W_{T_i}}}{\partial b_j^l} \end{aligned} \tag{13}$$

with

$$\begin{aligned} \frac{\partial f_i^{-1}}{\partial b_j^l} &= \begin{cases} -\left(\dfrac{\partial f_i}{\partial b_j^l} / f_i^{'}\right) \circ f_i^{-1} \neq 0 & \text{if } i = j \\ 0 & \text{if } i \neq j \end{cases} \\ \frac{\partial \tilde{f}_i}{\partial b_j^l} &= \begin{cases} K_{\Delta_i} \star \dfrac{\partial f_{i+1}}{\partial b_j^l} \neq 0 & \text{if } i+1 = j \\ 0 & \text{if } i+1 \neq j \end{cases} \end{aligned} \tag{14}$$

For clarity, using (14) as well as $\left(F'_{\mu_i} \circ \tilde{f}_i\right) \tilde{f}_i^{'} = F'_{W_{T_i}}$, we can simplify and rewrite the forward induction equations (13) as

$$\begin{aligned} \frac{\partial F_{\mu_i}}{\partial b_j^l} &= \begin{cases} 0 & \text{if } i < j \\ \left(\dfrac{\partial F_{W_{T_i^-}}}{\partial b_j^l} - F'_{W_{T_i^-}} \times \dfrac{\partial f_i}{\partial b_j^l} / f_i^{'}\right) \circ f_i^{-1} & \text{if } i = j \\ \dfrac{\partial F_{W_{T_i^-}}}{\partial b_j^l} \circ f_i^{-1} & \text{if } i > j \end{cases} \\ \frac{\partial F_{W_{T_i}}}{\partial b_j^l} &= \begin{cases} 0 & \text{if } i < j-1 \\ F'_{W_{T_i}} \times \dfrac{\partial \tilde{f}_i}{\partial b_j^l} / \tilde{f}_i^{'} & \text{if } i = j-1 \\ \dfrac{\partial F_{\mu_i}}{\partial b_j^l} \circ \tilde{f}_i & \text{if } i > j-1 \end{cases} \\ \frac{\partial F_{W_{T_{i+1}^-}}}{\partial b_j^l} &= \begin{cases} 0 & \text{if } i < j-1 \\ K_{\Delta_i} \star \dfrac{\partial F_{W_{T_i}}}{\partial b_j^l} & \text{if } i \geq j-1 \end{cases} \end{aligned} \tag{15}$$

Note that we have $F_{W_{T_0}}(w) = \mathbf{1}_{w\geq 0}$ and $F'_{W_{T_0}}(w) = \delta_{w=0}$, thus

$$\frac{\partial F_{W_{T_0}}}{\partial b_1^l}(w) = \left(\frac{\partial \tilde{f}_0}{\partial b_1^l}(0)/\tilde{f}_0'(0)\right)\delta_{w=0}$$

and

$$\frac{\partial F_{W_{T_1^-}}}{\partial b_1^l}(w) = \left(K_{\Delta_0} \star \frac{\partial F_{W_{T_0}}}{\partial b_j^l}\right)(w) = \left(\frac{\partial \tilde{f}_0}{\partial b_1^l}(0)/\tilde{f}_0'(0)\right)\frac{e^{-\frac{w^2}{2\Delta_0}}}{\sqrt{2\pi\Delta_0}}$$

is computed explicitly, with no need to regularize the Dirac function. Once we have all the $\frac{\partial F_{\mu_i}}{\partial b_j^l}$, it is straightforward to compute the expiry T_i and strike K vanilla call sensitivities as

$$\frac{\partial C(T_i,K)}{\partial b_j^l} = \int_K^{+\infty}(x-K)\,d\frac{\partial F_{\mu_i}}{\partial b_j^l}(x)$$

Note that $\frac{\partial F_{\mu_i}}{\partial b_j^l} \neq 0 \quad \forall j \leq i$ and $\frac{\partial F_{\mu_i}}{\partial b_j^l} = 0 \quad \forall j > i$ so that a vanilla option with expiry T_i has non-zero sensitivities to the b_j^l for all $j \leq i$ and zero sensitivities to the b_j^l for all $j > i$.

5.5. **Numerical examples.** Here we show the vega by expiry and strike computed using our Bass-LV model for the Autocall in Section 4.2.2 and the Asian in Section 4.2.3. For comparison we also plot the (exact) vega computed using a PDE solver (see [6] for an implementation).

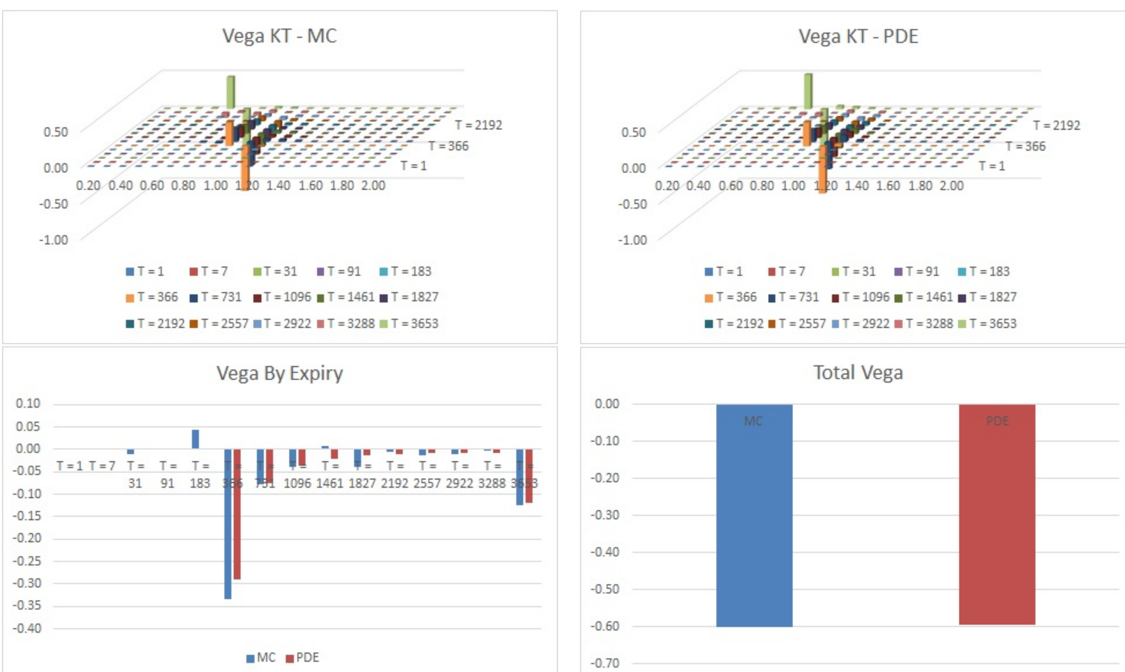

FIGURE 3. 10Y Autocall with yearly call dates, recall barrier 100 and PDI Barrier 70, incremental coupon 5.

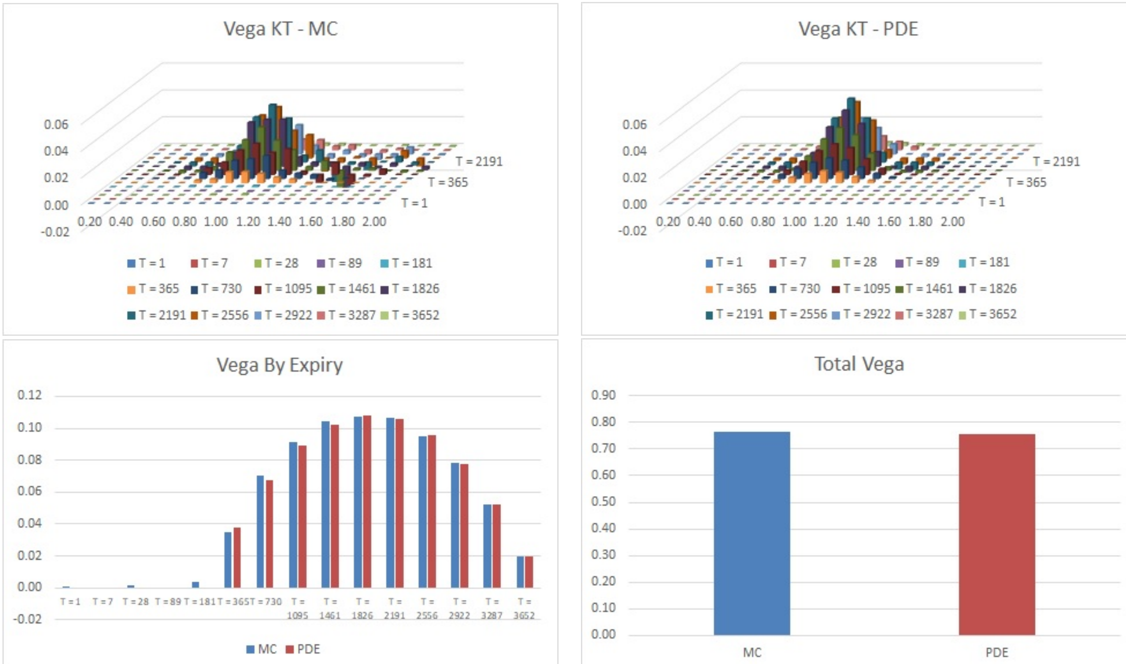

FIGURE 4. 10Y Asian option with yearly fixings and strike 100.

6. BASS^2 CONSTRUCTION: FITTING VANILLAS *and* FUTURE SKEWS

6.1. Bass construction with a general kernel K^X. We consider the following extension:

$$S_t = f_{[T_1,T_2]}(t, W_{T_1}, W_{T_1} + X_t), \forall\, t \in [T_1, T_2] \tag{16}$$

where $(X_t)_{T_1 \le t \le T_2}$ is now a generic one-dimensional diffusion, left unspecified for the moment, independent of W_{T_1}, with $X_{T_1} = 0$. Following closely Section 2, we derive:

Theorem 6.1. **(a)** *$(S_t)_{T_1 \le t \le T_2}$ is a martingale,* **(b)** *$S_{T_2} \sim \mu_2$ and* **(c)** *$S_{T_1} \sim \mu_1$ if and only if $F_{W_{T_1}}$ is the solution of the fixed-point equation:*

$$F_{W_{T_1}} = \mathcal{A}^X\, F_{W_{T_1}} \tag{17}$$

where the non-linear integral operator $\mathcal{A}^X : \mathcal{E} \to \mathcal{E}$ is defined by:

$$\mathcal{A}^X F := F_{\mu_1} \circ \left(K^{-X}_{T_2|X_{T_1}=0} \star \left(F^{-1}_{\mu_2} \circ \left(K^X_{T_2|X_{T_1}=0} \star F \right) \right) \right)$$

The mapping $f_{[T_1,T_2]}$ is then given by

$$f_{[T_1,T_2]}(t, w_1, w) = \left(K^{-X}_{T_2|X_t=w-w_1} \star \left(F^{-1}_{\mu_2} \circ \left(K^X_{T_2|X_{T_1}=0} \star F_{W_{T_1}} \right) \right) \right)(w_1)$$

$K^X_{T_2|X_t=x}$ is the kernel of the process $(X_t)_{T_1 \le t \le T_2}$, and we use the notation:

$$\left(K^{-X}_{T_2|X_t=x} \star f \right)(w) := \mathbb{E}\left[f(w + X_{T_2}) | X_t = x \right]$$
$$\left(K^{X}_{T_2|X_t=x} \star f \right)(w) := \mathbb{E}\left[f(w - X_{T_2}) | X_t = x \right]$$

Note that $f_{[T_1,T_2]}(T_2, w_1, w) = \left(F^{-1}_{\mu_2} \circ \left(K^X_{T_2|X_{T_1}=0} \star F_{W_{T_1}}\right)\right)(w)$ does not depend on w_1. Below we will use the notation

$$f_{[T_1,T_2]}(T_1, w) := f_{[T_1,T_2]}(T_1, w, w)$$
$$f_{[T_1,T_2]}(T_2, w) := f_{[T_1,T_2]}(T_2, w, w)$$

6.2. **Specifying a kernel K^X with the Bass construction.** We can specify a kernel K^X, easy to compute, using a one-marginal Bass construction (see Section 1) for which $X_t = \widetilde{f}(t, \widetilde{W}_t)$ with $\widetilde{W}_{T_1} := 0$ and such that $X_{T_2} \sim F'_{X_{T_2|X_{T_1}=0}}$ is specified so as to fit a future skew. This will be our choice below.

6.2.1. *Fitting a future skew.* From (16), an at-the-money digital option at time T_1 of maturity T_2 is given by

$$D(S_{T_1}) := \mathbb{E}[\mathbf{1}_{S_{T_2}<S_{T_1}}|S_{T_1}] = F_{X_{T_2|X_{T_1}=0}}\left(f^{-1}_{[T_1,T_2]}(T_2, S_{T_1}) - f^{-1}_{[T_1,T_2]}(T_1, S_{T_1})\right) \tag{18}$$

where $F_{X_{T_2|X_{T_1}=0}}$ is the cumulative distribution function of X_{T_2} conditional on $X_{T_1} = 0$. In practice, we take

$$D(S_{T_1}) = 1 + \frac{d}{dK}\mathrm{BS}\left(S_{T_1}, KS_{T_1}, \sigma_{[T_1,T_2]}(KS_{T_1})^2(T_2 - T_1)\right)|_{K=1}$$

where $\mathrm{BS}(S_0, K, v)$ denotes the Black-Scholes formula with spot S_0, strike K and variance v. The user chooses a specific future implied volatility $\sigma_{[T_1,T_2]}(KS_{T_1})$. We have therefore two unknowns $F_{W_{T_1}}, F_{X_{T_2|X_{T_1}=0}}$ for the two equations (17) and (18).

6.2.2. *Numerical algorithm.* The numerical algorithm can be described by the following steps:

(1) Inputs: Specify $\mu_1 \overset{\text{convex}}{<} \mu_2$ and $\sigma_{[T_1,T_2]}(\cdot)$;

(2) Choose a guess $F_{X_{T_2|X_{T_1}=0}} := F^{(p=0)}_{X_{T_2|X_{T_1}=0}}$;

(3) Using Algorithm (3.4.1), compute $F_{W_{T_1}}$ and the mappings $f_{[T_1,T_2]}(T_1, \cdot)$, $f_{[T_1,T_2]}(T_2, \cdot)$. Calculate $F^{(p+1)}_{X_{T_2|X_{T_1}=0}}$ using equation (18);

(4) Iterate step (3) until convergence of $F^{(p)}_{X_{T_2|X_{T_1}=0}}$. The convergence of our algorithm is not obvious.

6.3. **Specifying a kernel K^X with a stochastic volatility model.** Here we take for all $t \in [T_1, T_2]$,

$$S_t = f_{a_{T_1}}\left(t, W_{T_1} + a_{T_1}\left(\rho(B_t - B_{T_1}) + \sqrt{1-\rho^2}(B^\perp_t - B^\perp_{T_1})\right)\right)$$

where a_t is a stochastic volatility

$$da_t = b(a_t)dt + c(a_t)dB_t$$

with $(B_t)_{0\le t\le T}$ and $(B^\perp_t)_{0\le t\le T}$ two orthogonal Brownian Motions. In practice we use a stochastic volatility dynamics that can be simulated exactly, such as the exponential Ornstein-Uhlenbeck

$$a_t = a_0 \exp(\nu Z_t - \frac{1}{2}\nu^2 \mathrm{Var}[Z_t]), \quad dZ_t = -\lambda Z_t + dB_t, \quad Z_0 = 0$$

The dynamics for all $t \in [T_1, T_2]$ is then:

$$\frac{dS_t}{S_t} = \partial_w \ln f_{a_{T_1}}(t, f^{-1}_{a_{T_1}}(t, S_t))a_{T_1}\left(\rho dB_t + \sqrt{1-\rho^2}dB^\perp_t\right)$$

This corresponds to a (path-dependent) local stochastic volatility model. The mapping $f_{a_{T_1}}$ is built through the equations:

$$f(T_2, w) = F_{\mu_2}^{-1}\left(\mathbb{E}\left[F_{W_{T_1}}(w + a_{T_1}\sqrt{T_2 - T_1}G)\right]\right) \tag{19}$$

$$f_{a_{T_1}}(T_1, w) = \mathbb{E}\left[f(T_2, w + a_{T_1}\sqrt{T_2 - T_1}G)|a_{T_1}\right] \tag{20}$$

$$F_{\mu_1}(x) = \mathbb{E}\left[F_{W_{T_1}}(f_{a_{T_1}}^{-1}(T_1, x))\right] \tag{21}$$

and

$$f_{a_{T_1}}(t, w) = \mathbb{E}\left[f(T_2, w + a_{T_1}\sqrt{T_2 - t}G)|a_{T_1}\right]$$

where G is Gaussian. Note that the function $f_{a_{T_1}}$ does not depend on a_{T_1} at T_2.

6.3.1. *Numerical algorithm.* Solving equation (21) where the unknown is $F_{W_{T_1}}$ is not as easy as in the original martingale Bass construction. Below, we explain how to proceed. First, we note that equation (21) could be written as

$$F_{\mu_1}(x) = \mu_{W_{T_1}} \star \chi_f(\cdot, x), \quad \mu_{W_{T_1}} := F'_{W_{T_1}}, \quad \chi_f(w, x) := \mathbb{E}\left[\mathbf{1}_{x-w<f_{a_{T_1}}^{-1}(T_1,x)}\right]$$

By taking the Fourier transform (denoted by a hat symbol), we get

$$\hat{\mu}_{W_{T_1}}(k) = \frac{\hat{F}_{\mu_1}(k)}{\hat{\chi_f}(k, x)} \tag{22}$$

The calibration can be described by the following steps:

(1) Set $p = 0$ and choose $F_{W_{T_1}}^{(p)}$;
(2) Compute $f(T_2, w)$ with equation (19) for all w;
(3) Compute $f_{a_{T_1}}(T_1, w)$ with equation (20) for all w and a_{T_1};
(4) Compute χ_f and then $F_{W_{T_1}}^{(p+1)}$ with equation (22);
(5) Iterate steps (2-3-4) until convergence.

Appendix A. Proofs

Proof of 2.1. **(a)** As $(S_t)_{T_1 \le t \le T_2}$ is a martingale, we should have as in Section 1 that f is the solution of the heat kernel equation:

$$\partial_t f + \frac{1}{2}\partial_w^2 f = 0 \tag{23}$$

(b) The terminal condition $f(T_2, \cdot)$ arises from the constraint $S_{T_2} \sim \mu_2$:

$$\begin{aligned}
\mathbb{E}[\mathbf{1}_{S_{T_2}:=f(T_2,W_{T_2})\le f(T_2,w)}] &:= F_{\mu_2}(f(T_2, w)) = \mathbb{E}[\mathbf{1}_{W_{T_2}\le w}] \\
&= \mathbb{E}[\mathbb{E}[\mathbf{1}_{W_{T_1}+\sqrt{T_2-T_1}Z\le w}|Z]] \\
&= \mathbb{E}[F_{W_{T_1}}(w - \sqrt{T_2 - T_1}Z)] := K_{T_2-T_1} \star F_{W_{T_1}}(w)
\end{aligned}$$

with Z a standard Gaussian. We have used here that f is increasing in w. Hence $f(T_2, \cdot) = F_{\mu_2}^{-1} \circ \left(K_{T_2-T_1} \star F_{W_{T_1}}\right)$ and from the heat kernel equation (23), we have that the solution at $t = T_1$ reads:

$$f(T_1, \cdot) = K_{T_2-T_1} \star f(T_2, \cdot) = K_{T_2-T_1} \star \left(F_{\mu_2}^{-1} \circ \left(K_{T_2-T_1} \star F_{W_{T_1}}\right)\right) \tag{24}$$

(c) Similarly from the constraint $S_{T_1} \sim \mu_1$, we should have for all $w \in \mathbb{R}_+$:

$$\mathbb{E}[\mathbf{1}_{S_{T_1}:=f(T_1,W_{T_1})\le f(T_1,w)}] := F_{\mu_1}(f(T_1,w)) = \mathbb{E}[\mathbf{1}_{W_{T_1}\le w}] := F_{W_{T_1}}(w) \tag{25}$$

Putting together equations (24) and (25), $F_{W_{T_1}}$ is characterized as the solution of the fixed-point (1). The function $f(t,\cdot)$ for $t \in [T_1, T_2]$ is then given by (3). □

Proof of Theorem 2.1. **(a)** The set $\mathcal{E}$ is convex and closed. **(b)** From lemma 2.2, we have that $\mathcal{A}(\mathcal{E}) \subset \mathcal{E}$. **(c)** $\mathcal{A}$ is a continuous operator for the sup-norm and $\mathcal{A}(\mathcal{E})$ is relatively compact from Ascoli-Arzela's theorem as $\mathcal{A}(\mathcal{E})$ is uniformly bounded and Lipschitz ($F_{\mu_1}, F_{\mu_2}^{-1}, K_\Delta$ are Lipschitz). We conclude with the Schauder fixed point theorem. □

Proof of Proposition 2.5. **(a)** We deduce the general solution of (4), depending on a constant c_1 (one more can be eliminated from Remark 2.3 - **(2)** by imposing the condition $F^{-1}(\frac{1}{2}) = 0$):

$$F^{-1}(u) = \int_{\frac{1}{2}}^{u} dy \sqrt{\frac{G_2'(y)}{c_1 + \frac{2}{\Delta}\int_0^y (G_1(z) - G_2(z))dz}}$$

We must have $c_1 = 0$ so that $\lim_{u\to 1} F^{-1}(u) = \infty$ (note that $\int_0^1 (G_1(z) - G_2(z))dz = 0$). Finally, we obtain an unique solution:

$$F^{-1}(u) = \sqrt{\frac{\Delta}{2}} \int_{\frac{1}{2}}^{u} dy \sqrt{\frac{G_2'(y)}{\int_0^y (G_1(z) - G_2(z))dz}} \tag{26}$$

Note that $\int_0^y G_i(z)dz$, $i = 1, 2$ is directly related to asset or nothing digital calls through

$$\int_0^y G_i(z)dz = \int_{-\infty}^{G_i(y)} xF'_{\mu_i}(x)dx = \int_{-\infty}^{G_i(y)} x\mu_i(x)dx = \mathbb{E}\left[S_{T_i}\mathbf{1}_{S_{T_i}\le G_i(y)}\right]$$

(b) Note that the quantity $\int_0^y (G_1(z) - G_2(z))dz > 0$ if $\mu_1 \overset{\text{convex}}{<} \mu_2$. Indeed, we have

$$\begin{aligned}
\int_0^y (G_1(z) - G_2(z))dz &= \mathbb{E}[S_{T_1}\mathbf{1}_{S_{T_1}\le G_1(y)}] - \mathbb{E}[S_{T_2}\mathbf{1}_{S_{T_2}\le G_2(y)}] \\
&= \mathbb{E}[(G_2(y) - S_{T_2})\mathbf{1}_{Y\le G_2(y)}] - \mathbb{E}[(G_2(y) - S_{T_1})\mathbf{1}_{S_{T_1}\le G_1(y)}] \\
&= \mathbb{E}[(G_2(y) - S_{T_2})^+] - \mathbb{E}[(G_2(y) - S_{T_1})^+] \\
&\quad + \mathbb{E}[(G_2(y) - S_{T_1})\left(\mathbf{1}_{S_{T_1}\le G_2(y)} - \mathbf{1}_{S_{T_1}\le G_1(y)}\right)
\end{aligned}$$

The term $\mathbb{E}[(G_2(y) - S_{T_2})^+] - \mathbb{E}[(G_2(y) - S_{T_1})^+]$ is strictly positive by definition of the convex-order condition $\mu_1 \overset{\text{convex}}{<} \mu_2$. The payoff $(G_2(y) - S_{T_1})\left(\mathbf{1}_{S_{T_1}\le G_2(y)} - \mathbf{1}_{S_{T_1}\le G_1(y)}\right)$ is also obviously non-negative. Hence the convex-order condition implies $\int_0^y (G_1(z) - G_2(z))dz > 0$ as needed. □

References

[1] Bass, R.: *Skorokhod embedding via stochastic integrals*. In Jacques Azema and Marc Yor, editors, Séminaire de Probabilitées XVII 1981/82, number 986 in Lecture Notes in Mathematics, pages 221–224. 1983.

[2] Backhoff-Veraguas, J., Beiglbock, M., Huesmann, M., Sigrid Kallblad, S.: *Martingale Benamou–Brenier: a probabilistic perspective*, arXiv:1708.04869.

[3] Carr, P. , Geman, H., Madan, D.B., Yor, M.: From local volatility to local Lévy models, *Quantitative Finance*, Volume 4, Issue 5, 2004.

[4] Carr, P.: Local variance Gamma option pricing model, presentation, *IBCI Conference*, Paris (April 2009).

[5] Dupire, B.: Pricing with a smile, *Risk Magazine* 7, 18–20 (1994).

[6] Guennoun, H.: *Understanding autocalls: real time vega map*, SSRN 3387810 (2019).

[7] Guyon, J.: *Path-dependent volatility*, Risk magazine (Sept. 2014).

[8] Henry-Labordère, P.: *Calibration of Local Stochastic Volatility Models to Market Smiles: A Monte-Carlo Approach*, Risk Magazine, September 2009.
[9] Henry-Labordère, P.: *Model-free Hedging: A Martingale optimal transportation viewpoint*, Financial Mathematics Series CRC, Chapman Hall (190 p.), 2017.
[10] Henry-Labordère, P.: *From Schrödinger bridges to a new class of stochastic volatility models*, arXiv:1904.04554.
[11] Kellerer, H.G.: *Markov-Komposition und eine Anwendung auf Martingale*, Math. Ann., 198 (1972), p. 99 – 122.

Global Markets Quantitative Research, Natixis

Email address: antoine.conze-ext@natixis.com

Email address: pierre.henrylabordere@natixis.com